Jordan Journal of Mathematics and Statistics.
Yarmouk University

DOI:https://doi.org/10.47013/19.1.14

Enhanced Image Compression Via An Optimized Wavelet Thresholding Approach

A. M. Jarrah[1], *Abisha V*[2], *Ch Karam Nawaz*[2], *Pankaj Sharma*[2,*]

[1] Department of Mathematics, Yarmouk University, Irbid, Jordan and President, Philadelphia University, P. O. Box 1, 13932 Amman, Jordan
mail: ajarrah@yu.edu.jo; president@philadelphia.edu.jo
[2] Department of Mathematics, Pondicherry University, Puducherry - 605 014, India.

Received: April 30, 2025 Accepted: Sept. 30, 2025

Abstract: Image compression is crucial for reducing the size of digital images, particularly in applications such as medical imaging and satellite communication. Discrete Wavelet Transform (DWT) has emerged as a powerful tool for image compression due to its multiresolution analysis capabilities. In this study, we propose a novel thresholding technique for selecting optimal threshold values to enhance image compression using DWT. We evaluate the performance of our approach using different wavelets, including Haar, db2, db5, sym2, and coif1, and analyze key metrics such as Peak Signal-to-Noise Ratio (PSNR), Compression Score (CS), and L_2-norm recovery. Here, we show that for first level of decomposition using db2 wavelet, our proposed technique achieves a PSNR of 35.79 dB, a CS of 75%, and an L_2-norm recovery of 99.946% when applied to a standard 474×474 image of Srinivasa Ramanujan. Our method not only maintains image quality but reduces computational time compared to existing thresholding techniques. This work contributes to the advancement of efficient image compression techniques in various domains.

Keywords: Image Compression; Discrete Wavelet Transform (DWT); Thresholding; Multiresolution Analysis (MRA).

2010 Mathematics Subject Classification. 41A30; 42C15; 42C40.

1 Introduction

Digital Image Processing involves analyzing and manipulating digital images. Image compression is crucial for diminishing the size of images. Among its numerous applications, image compression appears as one of the most fruitful techniques for minimizing image size worldwide [14][33]. The challenge faced in image compression methods is to reduce the image data without affecting human visual perception and the statistical properties of image data [21][22]. Data compression techniques save storage space and faster transmission, reduces bandwidth usage, speeds up web page loading and download times, especially over networks [38]. Additionally, it improves performance, reduces costs and promotes accessibility in resource-limited systems. In applications wherever high-resolution images need to be stored or shared quickly with maintaining quality such as in multimedia, clinical imaging, satellite communication and other fields image compression plays a vital role [4].

There are various types of image compression methods namely Run Length Encoding, Arithmetic Coding, Huffman Encoding, LZW Coding, Discrete Cosine Transform, Discrete Fourier Transform, Discrete Wavelet Transform, Predictive Coding, Block Truncation Coding, Sub-band Coding, Fractal Compression, Singular Value Decomposition, Vector Quantization, and many more [12].

Minor dissimilarities in brightness over a large area are easily recognized by human vision, but not easy to examine the specific strength of a high frequency brightness variation [15][28]. In other words, the upper left corner of the eye is more sensitive to low frequencies and the lower right corner is less sensitive to high frequency [28]. Therefore, image

* Corresponding author e-mail: pankajsharma@pondiuni.ac.in

data can be reduced by discounting the high frequency components without compromising the vital feature of image [28]. The Discrete Wavelet Transform (DWT) is used as transformation tool because it can work in such a way like the human vision do [37] and it have become a significant method in signal processing, particularly for enhancing image performance in terms of Peak Signal to Noise Ratio (PSNR) [23][32]. An efficient compression scheme typically integrates multiple techniques, with wavelet transform being a prominent approach [7]. So, Methods involving Multiresolution Analysis (MRA) and wavelet transform is essential for efficiently representing image data. In MRA, image data is analysed at multiple resolutions, which separates fine details from coarse structures, helps in removing redundancy while preserving quality. In other hand, wavelets localize spatial and frequency information of an image data which helps us to capture features like textures and edges. Also, it compress the image with fewer coefficients, reducing usage of storage and bandwidth requirements while maintaining essential quality. Wavelet filters are designed to ensure that coefficients in each sub-band are nearly uncorrelated with those in other sub-bands [5]. Among image compression techniques, wavelet transform technique plays an important role in fields like medical imaging, satellite imaging and multimedia transmission where efficient compression and quality are vital.

In recent past, the image compression techniques involves mainly wavelet thresholding, Sureshrink, Bayesian, Adaptive threshold, redundant decomposition, translation invariant, Coefficient dependent, Double density dual tree complex DWT, Double density dual tree DWT, BM3D median filter DWT and many more [2].

Many researchers work on wavelet coefficient to reduce its size using various thresholding techniques [17][19][29][38]. In literature, a common approach in numerous Image Compression algorithms is to use a single threshold for all coefficients within a sub-band i.e. global thresholding [6]. Some researchers perform adaptive thresholding, which increases complexity and computational time [36]. Because of simplicity and efficiency global threshold concept is valuable. This method is not only easier to compute and implement but also more intuitive compared to complex adaptive or local thresholding methods. It reduces computational complexity, making it a fundamental tool in signal and image processing. During compression process, an optimal threshold value is used to separate important signal imformation from less relevant details. It determines the situation at which the wavelet coefficients are considered important enough to be retained, while coefficients below the threshold are discarded [26]. But, selection of this optimal threshold value(s) is one of the most challenging part and is crucial for achieving efficient compression and maintaining the quality of the compressed data [30]. Weak decision indicating threshold leads to a large amount of selected coefficients that turn out to insignificant decrease on compression ratio with longer computational time [10][20]. Calculating the optimal threshold value is very crucial since it need to analyze multiple data simultaneously [36]. Here, if the calculated threshold value is very small, it will absorb noise into signal. Whereas, if the calculated threshold value is too high, some important coefficients will be automatically discarded resulting an undesired image quality [7].

Numerous scholars have contributed to advancements in this domain, exploring various theoretical and practical aspects to enhance the field's understanding and applications. The optimal selection methods of fixed thresholds and adaptive thresholds under aperiodic signals [40], noise-insensitive signal adaptive threshold for ECG compression [34], interleaving compression scheme and an efficient threshold estimation algorithm so as to enhance the performance of ADTopk [41], improved two-dimensional maximum Shannon entropy median filter for the adaptive selection of a threshold to enhance the filter performance while stably and effectively retaining the details of the images [24] and novel top-down superpixel segmentation algorithm called Hierarchical Histogram Threshold Segmentation [35], have been proposed by many researchers.

In present paper, we proposed a novel algorithm to select the threshold value for image compression in wavelet domain. For verification, we applied this technique to a grayscale image of Srinivasa Ramanujan in five different wavelet environment such as Haar, Coiflet1 (coif1), Symlet2 (sym2), Daubechies2 (db2), and Daubechies5 (db5), and analysed peak signal to noise ratio (PSNR), compression score (CS) and L_2 norm recovery. We compared our results with other standard threshold selection techniques.

This paper is organized as follows: Section 2 presents some basic definitions and preliminaries relevant to our work. A novel algorithm for determining the threshold value is explained step by step in Section 3. In Section 4, the simulation parameters such as PSNR, CS and L_2 norm recovery are discussed. Finally, the conclusions are given in Section 5.

2 Preliminaries

2.1 Multiresolution Analysis (MRA)

Let $\{V_j\}_{j\in\mathbb{Z}}$ be a sequence of subspaces of $L^2(\mathbb{R})$. We say that $\{V_j\}_{j\in\mathbb{Z}}$ is a MRA of $L^2(\mathbb{R})$ [9], if

1. **Nested property:** $V_j \subset V_{j+1}$
2. **Density property:** $\overline{\bigcup_{j\in\mathbb{Z}} V_j} = L^2(\mathbb{R})$
3. **Separation property:** $\bigcap_{j\in\mathbb{Z}} V_j = \{0\}$
4. **Scaling property:** $f(t) \in V_0 \iff f(2^j t) \in V_j$
5. There exists a function $\phi \in V_0$, called the scaling function (Father wavelet), such that

$$\int_{\mathbb{R}} \phi(t)\,dt \neq 0$$

and $\{\phi(t-k)\}_{k\in\mathbb{Z}}$ forms an orthonormal basis for V_0.

2.2 Discrete Wavelet Transform

Let digital image $f(x,y)$ composed of N rows and M columns. A separable wavelet of $L^2(\mathbb{R}^2)$ is constructed using separable products of $\psi(t)$ and of $\phi(t)$, where $\phi(t)$ is connected to a 1-D multiresolution approximation V_j. Also,

– V_j^2 is the separable two dimensional multiresolution $V_j^2 = V_j \otimes V_j$
– W_j^2 is the detail space and $V_{j+1}^2 = V_j^2 \oplus W_j^2$

Here, $\psi(t)$ and $\phi(t)$ generate an orthonormal basis of $L^2(\mathbb{R})$. Further, three directional wavelets are:

$$\psi^1(x,y) = \phi(x)\psi(y) \tag{1}$$

$$\psi^2(x,y) = \psi(x)\phi(y) \tag{2}$$

$$\psi^3(x,y) = \psi(x)\psi(y) \tag{3}$$

where $\psi^1 = \psi^H$ shows the direction of the horizontal variations, $\psi^2 = \psi^V$ permits to detect the vertical variations, and $\psi^3 = \psi^D$ allows to detect the diagonal variations. The generic expression is

$$\psi^i_{j,m,n}(x,y) = 2^j \psi^i(2^j x - m, 2^j y - n),\ i = H,V,D \tag{4}$$

The directional wavelets $\psi^1_{j,m,n}, \psi^2_{j,m,n}, \psi^3_{j,m,n}$ forms an orthonormal basis of the subspace of details $W_j^2 = (V_j \otimes W_j) \oplus (W_j \otimes V_j) \oplus (W_j \otimes W_j)$ at scale j, with $L^2(\mathbb{R}^2) = \oplus_j W_j^2$, $\otimes$ denotes a tensor product [18]. The whole image $f(x,y)$ decompose as

$$f(x,y) = \sum_{j,m,n,i} d^i_{j,m,n} 2^j \psi^i_{j,m,n}(x,y), \text{ and} \tag{5}$$

$$d^i_{j,m,n} = \ < \psi^i_{j,m,n}, f(x,y) > \tag{6}$$

Eq. (6) detects the discrete wavelet coefficients of the test image as a function of the four (j,m,n,i) discrete variables.

An image $f(x,y)$ is decomposed into an approximation image (WT_ϕ), and the detail images corresponding to a horizontal (WT^H_ψ), a vertical (WT^V_ψ) and a diagonal (horizontal + vertical) (WT^D_ϕ), for each scale respectively, [18]:

$$WT_\phi(j) = a_j(x,y) = \ < f(x,y), \phi_j(x)\phi_j(y) > \tag{7}$$

$$WT^H_\psi(j) = d^H_j(x,y) = \ < f(x,y), \psi_j(x)\phi_j(y) > \tag{8}$$

$$WT^V_\psi(j) = d^V_j(x,y) = \ < f(x,y), \phi_j(x)\psi_j(y) > \tag{9}$$

$$WT^D_\psi(j) = d^D_j(x,y) = \ < f(x,y), \psi_j(x)\psi_j(y) > \tag{10}$$

In decomposition, the size of the image is divided by 2 at each iteration. Consequently, the representation of the wavelet coefficients can be seen as quarter-size subimages. Here, top left image corresponds to the approximation coefficients and other three images corresponds to the details coefficients [18]. Multilevel decomposition of the image using 2-D DWT is depicted in Figure 1.

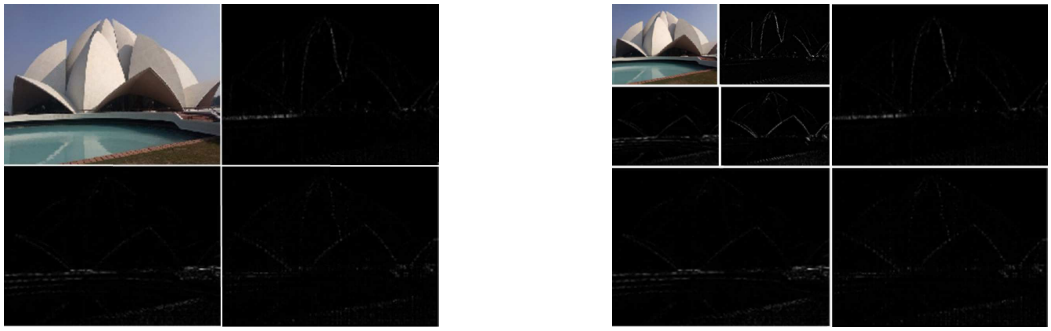

(a) First level decomposition **(b)** Second level decomposition

Fig. 1: 2-D Wavelet Decomposition.

2.3 Wavelet Families

Different families of wavelets are broadly used in image processing and analysis, each has its unique properties which make them suitable for particular applications. Present study investigates the importance of proposed thresholding technique using five well-known wavelets namely Haar, Daubechies 2 (db2), Symlet 2 (sym2), Coiflet 1 (coif1) and Daubechies 5 (db5) which are shown in Figure 2.

2.3.1 Haar Wavelet

The Haar wavelet function $\psi(t)$ can be described as

$$\psi(t) = \begin{cases} 1 & 0 \leq t < \frac{1}{2}, \\ -1 & \frac{1}{2} \leq t < 1, \\ 0 & \text{otherwise.} \end{cases}$$

Its scaling function $\varphi(t)$ can be described as [9]

$$\varphi(t) = \begin{cases} 1 & 0 \leq t < 1, \\ 0 & \text{otherwise.} \end{cases}$$

2.3.2 db2 and db5

The Daubechies family are written as dbN, where N is the order of the wavelet. The order is the number of vanishing moments for the particular Daubechies wavelet [9]. A wavelet has N vanishing moments if $\int_{-\infty}^{\infty} t^k \psi(t)dt = 0, \quad \text{for} \quad 0 \leq k < N$. db2 wavelet has 2 vanishing moments and Daubechies wavelet of order 5 has five vanishing moments, which is more complex wavelet with a longer support compared to db2. It has 10 coefficients in its scaling and wavelet filters. The Daubechies wavelet of order 5 offers a better balance between time and frequency localization than db2, which is useful for applications requiring finer detail preservation. More detailed with five vanishing moments, suitable for applications requiring higher precision and better time-frequency localization [13].

2.3.3 coif1

An orthonormal wavelet ψ with compact support is known as coiflet of order N, if the following conditions are satisfied. *i)* $\int_{-\infty}^{\infty} \psi(x)dx = 0$ *ii)* $\int_{-\infty}^{\infty} \phi(x)dx = 1$. Here, ϕ is the scaling funtion corresponding to ψ [8].

2.3.4 sym2

The construction of symlet wavelets basis is similar to the construction of Daubechies wavelets bases. Symlet wavelets are symmetric. The Daubechies wavelets have maximial phase, whereas the Symlet have minimal phase [39]. Symelet wavelet (sym) has been applied for sound recognition systems. The Symlet wavelet is especially useful in applications requiring symmetry and orthogonality, such as image compression, signal processing, and feature extraction [1].

Each of these wavelets has specific properties regarding frequency response, vanishing moments, support, and other characteristics that make them suitable for different types of signal analysis, compression and feature extraction tasks. The choice of wavelet depends on the specific requirements and characteristics of the signal being analysed or processed. Therefore, we have used these wavelets in the current paper.

2.4 Pixel

Pixel is the fundamental element of a digital image. It is a small rectangle that ranges in grayscale from black to white [9].

2.4.1 Neighbours of a Pixel

Digital grayscale images are represented as a table of $n \times m$ pixels. Consider pixel 'p' at coordinates (x,y). It has four horizontal and vertical neighbours whose coordinates are given by $(x+1,y),(x-1,y),(x,y+1),(x,y-1)$ [27]. This set of pixels, called the 4-neighbours of p, and it is denoted as $\mathcal{N}_4(p)$. If (x, y) lies on the boundary of the digital image, some of the neihgbours of p lies outside the image. The four diagonal neighbours of 'p' have coordinates $(x+1,y+1),(x+1,y-1),(x-1,y+1),(x-1,y-1)$ and denoted by $\mathcal{N}_D(p)$ [27].

In Figure 3a, 3b show $\mathcal{N}_4(p)$ and $\mathcal{N}_D(p)$. It is together giving 8-neighbours of 'p', denoted by $\mathcal{N}_8(p)$ [27].

2.4.2 Distance Measure

For pixels $p(x,y)$, $q(s,t)$, and $z(v,w)$, satisfying following conditions is called distance function or metric [27].

1. $D(p,q) > 0$ and $D(p,q) = 0$ if and only if $p = q$.
2. $D(p,q) = D(q,p)$ (Symmetry).
3. $D(p,z) \leq D(p,q) + D(q,z)$ (Triangle inequality).

2.5 Thresholding

In image processing, we generally require image segmentation. One of the processes of image segmentation in digital image processing is known as thresholding [25].

2.5.1 Hard Thresholding

A hard thresholding function is defined as [31]

$$h(x) = \begin{cases} x, & \text{if } |x| > T, \\ 0, & \text{if } |x| \leq T. \end{cases}$$

Where T is threshold value.

2.5.2 Soft Thresholding

It is defined by the function [3]

$$s(x) = \begin{cases} sign(x) \cdot (|x| - T), & \text{if } |x| \geq T, \\ 0, & \text{if } |x| < T. \end{cases}$$

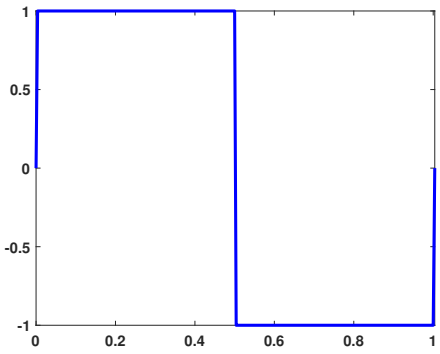

(a) Haar Wavelet function

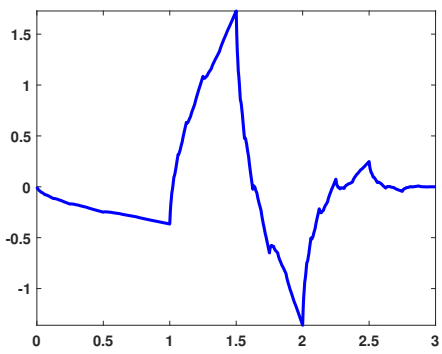

(b) Daubechies 2 Wavelet function

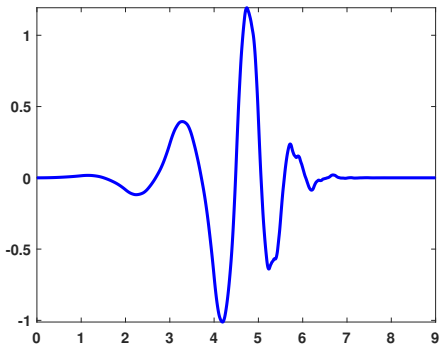

(c) Daubechies 5 Wavelet function

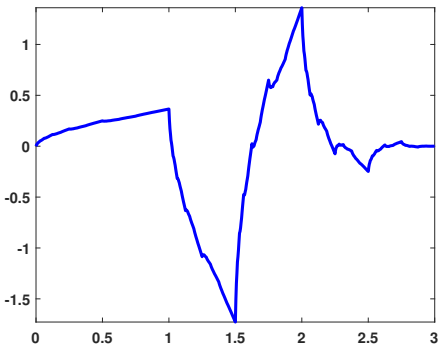

(d) Symlet 2 Wavelet function

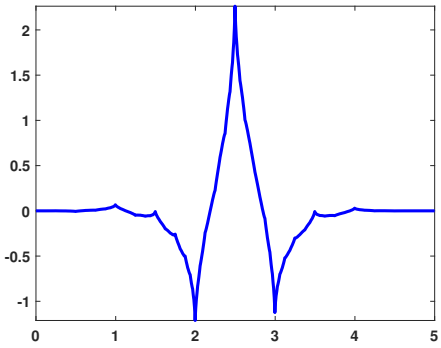

(e) Coiflet 1 Wavelet function

Fig. 2: Different Wavelets.

2.5.3 Global Thresholding

Let $f(x,y)$ be a pixel in 2-D image. The segmented image $g(x,y)$ is defined as [22]

$$g(x,y) = \begin{cases} 1 & \text{if } f(x,y) > T, \\ 0 & \text{if } f(x,y) \leq T. \end{cases}$$

When 'T' is a constant that is applied to the entire image, the process is known as global thresholding.

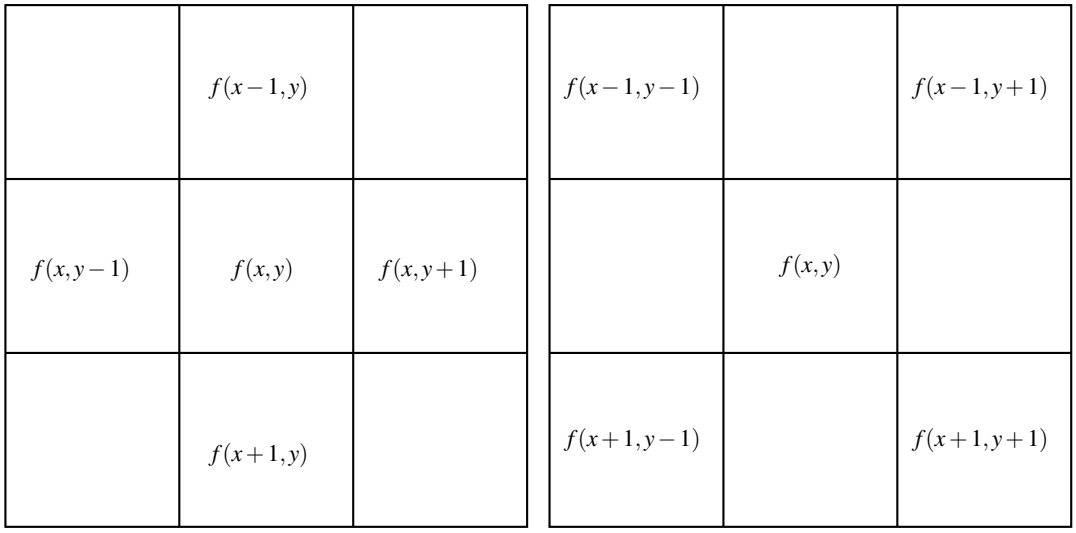

(a) 4-neighbours of a pixel $\mathcal{N}_4(p)$. **(b)** Four diagonal neighbours of a pixel $\mathcal{N}_D(p)$.

Fig. 3: Neighbours of a Pixel

– *VisuShrink.* It was introduced by Donoho and defined as $\sigma\sqrt{2\log N}$ where σ is the noise variance and N is the number of pixels in the image [11].
– *Ostu Method.* In this method, let (x,y) denote the spatial coordinate of a digitized image, $G=\{0,1,...,L-1\}$ be a set of positive integers representing gray levels and n_i be the number of pixels with gray level i.
Then

$$n=\sum_{i=0}^{L-1} n_i$$

gives the total number of pixels in a given test image.
And the probability of occurrence of gray level i is obtained as

$$p_i=\frac{n_i}{n}.$$

In this method [25], to compute threshold operation, we partition pixels of the test image into two classes C_0 and C_1 (i.e., objects and background) at gray level t. Where, $C_0=\{0,1,\ldots,t\}$ and $C_1=\{t+1,t+2,\ldots,L-1\}$.

Let σ_w^2, σ_B^2, and σ_t^2 be within-class variance, between-class variance, and total variance, respectively [25]. An optimal threshold value can be determined by minimizing one of the following criterion with respect to t:

$$\lambda=\frac{\sigma_B^2}{\sigma_W^2},\quad \eta=\frac{\sigma_B^2}{\sigma_T^2},\quad \text{and}\quad \kappa=\frac{\sigma_T^2}{\sigma_W^2}.$$

Among three criterion, η is the simplest one. Thus, the optimal threshold t^* is calculated as

$$t^*=\underset{t\in G}{ArgMin}\,\eta,$$

where

$$\sigma_T^2=\sum_{i=0}^{L-1}(i-\mu_T)^2 p_i,\quad \mu_T=\sum_{i=0}^{L-1} i p_i$$

$$\sigma_B^2=\omega_0\omega_1(\mu_1\mu_0)^2,\quad \omega_0=\sum_{i=0}^{t} p_i,\quad \omega_1=1-\omega_0,$$

$$\mu_1 = \frac{\mu_T - \mu_t}{1-\omega_0},\ \mu_0 = \frac{\mu_t}{\omega_0},\ \mu_t = \sum_{i=0}^{t} i p_i,$$

– *Minimum Error Method.* In this method [25], the probability density function $p(g)$ of the test image comprising the gray levels of the object and background pixels. It is assumed that each of the two components $p(g|i)$ is normally distributed with mean μ_i, standard deviation σ_i, and a prior probability P_i [25], i.e.

$$p(g) = \sum_{i=1}^{2} P_i\, p(g|i)$$

where

$$p(g|i) = \frac{1}{\sqrt{2\pi}\sigma_i} \exp\left(-\frac{(g-\mu_i)}{2\sigma_i^2}\right).$$

The threshold value can be selected by solving the quadratic equation

$$\frac{(g-\mu_1)^2}{\sigma_1^2} + \log_e \sigma_1^2 - 2\log_e P_1 = \frac{(g-\mu_2)^2}{\sigma_2^2} + \log_e \sigma_2^2 - 2\log_e P_2$$

However, the parameters μ_i, σ_i^2 and P_i for $i = 1,2$ of $p(g)$ associated with an image (to be thresholded) are not known usually. To overcome this authors in [16], introduced another function $J(t)$, which is given by:

$$J(t) = 1 + 2\{P_1(t)\log_e \sigma_1(t) + P_2(t)\log_e \sigma_2(t)\} - 2\{P_1(t)\log_e P_1(t) + P_2(t)\log_e P_2(t)\}$$

where

$$P_1(t) = \sum_{g=0}^{t} h(g), \quad P_2(t) = \sum_{g=t+1}^{L-1} h(g),$$

$$\mu_1(t) = \frac{\sum_{g=0}^{t} h(g)g}{P_1(t)} \quad \mu_2(t) = \frac{\sum_{g=t+1}^{L-1} h(g)g}{P_2(t)}$$

$$\sigma_1^2(t) = \frac{\sum_{g=0}^{t} (g-\mu_1(t))^2 h(g)}{P_1(t)}$$

and

$$\sigma_2^2(t) = \frac{\sum_{g=t+1}^{L-1} (g-\mu_2(t))^2 h(g)}{P_2(t)}$$

The optimal threshold value is then obtained by minimizing $J(t)$, i.e., by finding

$$t^* = \underset{t \in G}{ArgMin}\, J(t).$$

– *rem_n0.* It gives a threshold value close to zero. Threshold value is median of absolute value of the coefficients.
– *bal_sn.* It gives a threshold value in such a way that the percentages of retained energy is equal to the number of zeros.

2.6 Image Compression Algorithm

1. *Wavelet decomposition.* Apply DWT by choosing a wavelet and a level of decomposition N. In this paper, we choose five different wavelets as mentioned earlier and first decomposition level as well as second decomposition level.
2. *Threshold detail coefficients.* For each level, a threshold value is selected and it is applied to the detail coefficients.
3. *Compressed Image.* Compute Inverse DWT using the original approximation coefficients of level N and the modified detail coefficients to obtain compressed image.

Figure 4 shows the block diagram of the proposed algorithm.

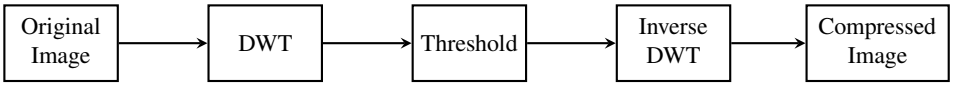

Fig. 4: The block diagram of image compression process.

2.7 Measurements of Image Quality

2.7.1 Mean Square Error (MSE)

The MSE can be calculated using the following formula

$$\text{MSE} = \frac{1}{nm}\sum_{j=0}^{n-1}\sum_{i=0}^{m-1}|X(i,j) - X_c(i,j)|^2 \tag{11}$$

Here,

- $n \times m$ represents the dimensions of image.
- $X(i,j)$ represents the given digital image.
- $X_c(i,j)$ represents the compressed image.

2.7.2 Peak Signal to Noise Ratio (PSNR)

In lossy compression, the compressed image's pixel values differ from the original image's pixel values. If the difference between the original and compressed images is imperceptible to the human eye, it signifies good compression. In this study, PSNR (which serve as a metric to quantify peak error) has been used to measure the quality of the compressed image. Its relevance is constrained to data encoded as bits per sample or bits per pixel. A higher PSNR value corresponds to enhanced quality in the compressed image. The following equation defines the PSNR:

$$\text{PSNR} = 10 \cdot \log_{10}\left(\frac{\text{max}^2}{\text{MSE}}\right), \tag{12}$$

where max represents the color depth.

2.7.3 Compression Score (CS)

Compression score, returned as a real number which is the percentage of thresholded coefficients that are equal to 0. It indicates how much of the original image data is retained after compression. It is often expressed as a percentage of retained wavelet coefficients.

2.7.4 L_2 Norm Recovery

$$L_2 \text{ norm recovery} = 100 \times \left(\frac{\|CXC\|}{\|C\|}\right)^2,$$

where

- C denotes the wavelet expansion coefficients of the given image.
- X is the test image.
- CXC represents the wavelet expansion coefficients of compressed image.

The L_2 norm recovery measures how well the compressed image retains the energy (or intensity) of the original image.

3 Proposed Threshold Technique

Let $\alpha_{x,y}$ denotes the pixel value at the spatial coordinate (x, y) of a digitized image. To compute threshold operation, first break the matrix of an image into 3×3 block matrices.

For $i \equiv 1 \pmod 3$ and $j \equiv 1 \pmod 3$, the optimal threshold value is proposed by

$$th^p = \max_{\substack{1\le i\le n\\ 1\le j\le m}} \left(\frac{\sum_{a=i}^{i+2}\sum_{b=j}^{j+2} |\alpha_{a,b} - \alpha_{i+1,j+1}|}{8} \right)$$

where $\alpha_{i+1,j+1}$ is the centre node of the block matrix

$$\begin{bmatrix} \alpha_{i,j} & \alpha_{i,j+1} & \alpha_{i,j+2} \\ \alpha_{i+1,j} & \alpha_{i+1,j+1} & \alpha_{i+1,j+2} \\ \alpha_{i+2,j} & \alpha_{i+2,j+1} & \alpha_{i+2,j+2} \end{bmatrix}.$$

3.1 Algorithm

In this paper we took an image of size $n \times m$.

Step 1: If n and m are divisible by 3, proceed to step 2, if not, examine the size of the matrix $n_1 \times m_1$ as follows $n_1 = 3 \times [\frac{n}{3}]$ and $m_1 = 3 \times [\frac{m}{3}]$.

1. If n or $m \cong 1(mod 3)$, remove any boundary row or column.
2. If n or m $\cong 2(mod 3)$, remove both the boundaries of the row or columns.

Step 2: Consider the resultant matrix and break it into 3×3 block matrix. For example 12×9 matrix is divided into block matrices as follows,

$$\left[\begin{array}{ccc|ccc|ccc} \alpha_{1,1} & \alpha_{1,2} & \alpha_{1,3} & \alpha_{1,4} & \alpha_{1,5} & \alpha_{1,6} & \alpha_{1,7} & \alpha_{1,8} & \alpha_{1,9} \\ \alpha_{2,1} & \alpha_{2,2} & \alpha_{2,3} & \alpha_{2,4} & \alpha_{2,5} & \alpha_{2,6} & \alpha_{2,7} & \alpha_{2,8} & \alpha_{2,9} \\ \alpha_{3,1} & \alpha_{3,2} & \alpha_{3,3} & \alpha_{3,4} & \alpha_{3,5} & \alpha_{3,6} & \alpha_{3,7} & \alpha_{3,8} & \alpha_{3,9} \\ \hline \alpha_{4,1} & \alpha_{4,2} & \alpha_{4,3} & \alpha_{4,4} & \alpha_{4,5} & \alpha_{4,6} & \alpha_{4,7} & \alpha_{4,8} & \alpha_{4,9} \\ \alpha_{5,1} & \alpha_{5,2} & \alpha_{5,3} & \alpha_{5,4} & \alpha_{5,5} & \alpha_{5,6} & \alpha_{5,7} & \alpha_{5,8} & \alpha_{5,9} \\ \alpha_{6,1} & \alpha_{6,2} & \alpha_{6,3} & \alpha_{6,4} & \alpha_{6,5} & \alpha_{6,6} & \alpha_{6,7} & \alpha_{6,8} & \alpha_{6,9} \\ \hline \alpha_{7,1} & \alpha_{7,2} & \alpha_{7,3} & \alpha_{7,4} & \alpha_{7,5} & \alpha_{7,6} & \alpha_{7,7} & \alpha_{7,8} & \alpha_{7,9} \\ \alpha_{8,1} & \alpha_{8,2} & \alpha_{8,3} & \alpha_{8,4} & \alpha_{8,5} & \alpha_{8,6} & \alpha_{8,7} & \alpha_{8,8} & \alpha_{8,9} \\ \alpha_{9,1} & \alpha_{9,2} & \alpha_{9,3} & \alpha_{9,4} & \alpha_{9,5} & \alpha_{9,6} & \alpha_{9,7} & \alpha_{9,8} & \alpha_{9,9} \\ \hline \alpha_{10,1} & \alpha_{10,2} & \alpha_{10,3} & \alpha_{10,4} & \alpha_{10,5} & \alpha_{10,6} & \alpha_{10,7} & \alpha_{10,8} & \alpha_{10,9} \\ \alpha_{11,1} & \alpha_{11,2} & \alpha_{11,3} & \alpha_{11,4} & \alpha_{11,5} & \alpha_{11,6} & \alpha_{11,7} & \alpha_{11,8} & \alpha_{11,9} \\ \alpha_{12,1} & \alpha_{12,2} & \alpha_{12,3} & \alpha_{12,4} & \alpha_{12,5} & \alpha_{12,6} & \alpha_{12,7} & \alpha_{12,8} & \alpha_{12,9} \end{array}\right].$$

Step 3: For each 3×3 block matrix, find the centre node.

Step 4: Calculate the difference between central node and their 8-neighbouring node pixel values of the chosen block matrix.

Step 5: Calculate $A_{i,j} = \frac{\sum_{a=i}^{i+2}\sum_{b=j}^{j+2} |\alpha_{a,b} - \alpha_{i+1,j+1}|}{8}$.

Step 6: Repeat the steps 2 to 5 for all the block matrices.

Step 7: For $i \equiv 1 \pmod 3$ and $j \equiv 1 \pmod 3$

$$\text{Proposed threshold value } (th^p) = \max_{\substack{1\le i\le n\\ 1\le j\le m}} (A_{i,j}).$$

4 Results and Discussion

We applied proposed thresholding technique on a test image (Ramanujan image) of size 474×474. The technique is analysed upto second level of wavelet decomposition. Performance analysis using five wavelets such as Haar, sym2, db2, db5 and coif1 is studied to verify the superiority of the proposed technique.

After first level wavelet decomposition of the test image, we get averages (LL), vertical differences (HL), horizontal differences (LH) and diagonal differences (HH), the threshold value is then selected using proposed threshold technique. We used this threshold value on the detail coefficients (LH, HL, HH). Finally, inverse DWT is applied using approximate coefficients together with the modified detail coefficients we get the compressed image (O/p Image) which is shown in Figures 5 - 9.

(a) Haar LL **(b)** Haar LH **(c)** Haar HL **(d)** Haar HH **(e)** O/p Image

Fig. 5: First Level Haar Wavelet Decomposition.

(a) db2 LL **(b)** db2 LH **(c)** db2 HL **(d)** db2 HH **(e)** O/p Image

Fig. 6: First Level db2 Wavelet Decomposition.

(a) db5 LL **(b)** db5 LH **(c)** db5 HL **(d)** db5 HH **(e)** O/p Image

Fig. 7: First Level db5 Wavelet Decomposition.

Since, *visushrink* gives $8.6590e^{-06} \approx 0$ as a threshold value, therefore, it is not advisable to consider this value for any comparative analysis. Tables 1 - 10 show that *Minimum Error Threshold* and *rem_n*0 methods give good PSNR but compression score is very less compared to other methods. Therefore such methods may not be applicable, where we

(a) coif1 LL **(b)** coif1 LH **(c)** coif1 HL **(d)** coif1 HH **(e)** O/p Image

Fig. 8: First Level coif1 Wavelet Decomposition.

(a) sym2 LL **(b)** sym2 LH **(c)** sym2 HL **(d)** sym2 HH **(e)** O/p Image

Fig. 9: First Level sym2 Wavelet Decomposition.

Threshold Techniques	**Threshold Value**	**PSNR**	**CS**	L_2 **Norm**
Otsu's Method	0.4667	32.8232	75	99.8447
Proposed Method	**0.3054**	**32.8232**	**75**	**99.8447**
Minimum Error Threshold	0.023	43.1799	66.4837	99.986
*rem_n*0	0.0039	64.1321	37.3231	99.9998
bal_sn	0.2863	32.8232	75	99.8447

Table 1: First Level Haar Wavelet Decomposition.

Threshold Techniques	**Threshold Value**	**PSNR**	**CS**	L_2 **Norm**
Otsu's Method	0.4667	26.94	93.6114	99.5379
Proposed Method	**0.3054**	**27.4359**	**93.4648**	**99.6279**
Minimum Error Threshold	0.023	43.3124	78.5864	99.9818
*rem_n*0	0.0039	63.6522	43.4388	99.9998
bal_sn	0.8225	26.1942	93.71	99.382

Table 2: Second Level Haar Wavelet Decomposition.

Threshold Techniques	**Threshold Value**	**PSNR**	**CS**	L_2 **Norm**
Otsu's Method	0.4667	35.7901	75	99.946
Proposed Method	**0.3054**	**35.7901**	**75**	**99.946**
Minimum Error Threshold	0.023	42.4901	70.5057	99.9872
*rem_n*0	0.0039	58.8274	47.6767	99.9995
bal_sn	0.7564	35.7901	75	99.946

Table 3: First Level db2 Wavelet Decomposition.

need high image quality with better compression score. That is why in the present paper we are not considering these results for comparative analysis.

Threshold Techniques	**Threshold Value**	**PSNR**	**CS**	L_2 **Norm**
Otsu's Method	0.4667	26.3708	93.6572	99.7192
Proposed Method	**0.3054**	**27.2113**	**93.5495**	**99.7817**
Minimum Error Threshold	0.023	43.4206	83.4221	99.9825
*rem_n*0	0.0039	58.2279	53.7278	99.9994
bal_sn	0.7564	26.623	93.6708	99.7003

Table 4: Second Level db2 Wavelet Decomposition.

Threshold Techniques	**Threshold Value**	**PSNR**	**CS**	L_2 **Norm**
Otsu's Method	0.4667	33.4092	75	99.9743
Proposed Method	**0.3054**	**33.4092**	**75**	**99.9743**
Minimum Error Threshold	0.023	40.9406	72.729	99.9892
*rem_n*0	0.0039	56.8159	50.2445	99.9994
bal_sn	0.1819	33.4092	75	99.9743

Table 5: First Level db5 Wavelet Decomposition.

Threshold Techniques	**Threshold Value**	**PSNR**	**CS**	L_2 **Norm**
Otsu's Method	0.4667	26.6177	93.3949	99.8162
Proposed Method	**0.3054**	**32.0226**	**93.3949**	**99.8162**
Minimum Error Threshold	0.023	39.9124	85.7711	99.9825
*rem_n*0	0.0039	56.4115	56.4735	99.9994
bal_sn	0.591	32.0506	93.3996	99.8112

Table 6: Second Level db5 Wavelet Decomposition.

Threshold Techniques	**Threshold Value**	**PSNR**	**CS**	L_2 **Norm**
Otsu's Method	0.4667	32.7136	75	99.9497
Proposed Method	**0.3054**	**32.7136**	**75**	**99.9497**
Minimum Error Threshold	0.023	41.0744	70.7056	99.9871
*rem_n*0	0.0039	59.088	47.3031	99.9995
bal_sn	0.2019	32.7136	75	99.9497

Table 7: First Level coif1 Wavelet Decomposition.

Threshold Techniques	**Threshold Value**	**PSNR**	**CS**	L_2 **Norm**
Otsu's Method	0.4667	24.7191	93.5335	99.74
Proposed Method	**0.3054**	**24.498**	**93.3418**	**99.7991**
Minimum Error Threshold	0.023	24.498	93.4318	99.7991
*rem_n*0	0.0039	58.5514	53.6291	99.9995
bal_sn	0.7346	24.46	93.5539	99.7141

Table 8: Second Level coif1 Wavelet Decomposition.

Threshold Techniques	**Threshold Value**	**PSNR**	**CS**	L_2 **Norm**
Otsu's Method	0.4667	35.7901	75	99.946
Proposed Method	**0.3054**	**35.7901**	**75**	**99.946**
Minimum Error Threshold	0.023	42.4901	70.7057	99.9872
*rem_n*0	0.0039	58.8274	47.6767	99.9995
bal_sn	0.2793	35.7901	75	99.946

Table 9: First Level sym2 Wavelet Decomposition.

Threshold Techniques	Threshold Value	PSNR	CS	L_2 Norm
Otsu's Method	0.4667	26.3708	93.6572	99.7192
Proposed Method	**0.3054**	**27.2113**	**93.5495**	**99.7817**
Minimum Error Threshold	0.023	43.4206	83.4221	99.9825
rem_n0	0.0039	58.2279	53.7278	99.9994
bal_sn	0.7564	26.623	93.6708	99.7003

Table 10: Second Level sym2 Wavelet Decomposition.

Threshold Techniques	Time (in sec)
Otsu's Method	2.6406
Proposed Method	**1.1093**
bal_sn	4.0156

Table 11: Computational Time (Machine configuration is: 12th Gen Intel(R) Core(TM) i5-12450H 2.00 GHz, 8GB RAM).

In almost all the experiments, we note that while measuring PSNR, CS and L_2 norm recovery, our proposed technique gives not only similar PSNR and CS, but gives better L_2 norm recovery. Hence, the proposed threshold value selection technique show superiority over existing thresholding techniques. Also, compare other algorithms, the proposed technique in present paper yields less computational time which is shown in Table 11.

5 Conclusion

In this paper, a new threshold selection technique is proposed for image compression by preserving the quality of the image, which is based on pixel neighbourhood concept. Experiments are conducted to assess the performance of the proposed threshold selection technique in comparison with the existing threshold selection techniques. The results show that the proposed technique gives not only better L_2 norm recovery but it takes less computational time, compare to other existing methods.

Declarations

Competing interests: The authors declare that they have no Conflict of interest.
Authors' contributions: All authors contribute equally to this work.
Funding: The authors declare that no funds were received during the preparation of this manuscript.
Acknowledgments: Authors[2] are thankful to the DST, Government of India, India, under FIST program (Ref. SR/FST/MS-I/2024/173) for providing research facilities towards the completion of this paper.

References

[1] A. Glowacz, Diagnostics of Direct Current machine based on analysis of acoustic signals with the use of symlet wavelet transform and modified classifier based on words, *Eksploatacja i Niezawodność - Maintenance and Reliability*, **16**(2014), 554-558.
[2] A. Halidou, Y. Mohamadou, A. Ari, E. Zacko, Review of wavelet denoising algorithms, *Multimedia Tools and Applications*, **82**(2023), 1-31.
[3] A. Phinyomark, C. Limsakul, P. Phukpattaranont, A Comparative Study of Wavelet Denoising for Multifunction Myoelectric Control, *International Conference on Computer and Automation Engineering, Bangkok, Thailand*, (2009), 21-25.
[4] B. Das, A. Saha, S. Sikder, A Novel Image Compression Technique and Secured Transmission of Compressed Satellite Images Via Optical Fiber Using 6D Hyper Chaos, *J Indian Soc Remote Sens.*, **53**(2025), 511-530.
[5] B. Usevitch, A tutorial on modern lossy wavelet image compression: Foundations of JPEG 2000, *Signal Processing Magazine, IEEE*, **18**(2001), 22 - 35.
[6] C.S.Ahmed, F.B.Reguig, S.Ahmaidi, O.Fokapu, Wavelet denoising of the electrocardiogram signal based on the corrupted noise estimation, *Computers in Cardiology*, **32**(2005), 1021-1024.

[7] C. Zhen, Y. Su, Research on Wavelet image threshold denoising, *Int. Conf. Futur. Power Energy Eng.*, (2010), 3-6.
[8] D. Černá, V. Finěk, K. Najzar, On the exact values of coefficients of coiflets, *centr.eur.j.math.*, **6**(2008), 159-169.
[9] D. Ruch, P. Flett, Wavelet Theory: An elementary approach with application, (2011).
[10] F.A. Llinas, 2-Step scalar deadzone quantization for bitplane image coding, *IEEE Trans Image Process*, **22(12)**(2013), 4678-4688.
[11] F. Xiao, Y. Zhang, A comparative study on thresholding methods in wavelet-based Image Denoising, *Procedia Engineering*, **15**(2011), 3998-4003.
[12] G. Garg, R. Kumar, Analysis of different image compression techniques: A review, *Proceedings of the International Conference on Innovative Computing and Communication (ICICC)*, (2022).
[13] G. Lindfield, J. Penny, Analyzing data using discrete transforms, Numerical Methods (Fourth Edition), *Academic Press.*, (2019), 383-431.
[14] G.S. Kumar, M.L.P. Rani, Image Compression Using Discrete Wavelet Transform and Convolution Neural Networks, *J. Electr. Eng. Technol.*, **19**(2024), 3713-3721.
[15] G. Teng, R. Jiang, X. Liu, et al., EARN: toward e cient and robust JPEG compression artifact reduction, *Vis Comput.*, **40**(2024), 3033-3053.
[16] J. Kittler, J. Illingworth, Minimum error thresholding, *Pattern Recognit.*, **19**(1986), 41-47.
[17] L.C. Kho, Y. Tan, Y. Lim, Joint LZW and lossless dictionary-based bit-packing compression techniques for congested network, *IC4T*, (2015).
[18] L. Navarro, G. Courbebaisse, M. Jourlin, Chapter two - Logarithmic wavelets, *Advances in Imaging and Electron Physics, Elsevier*, **183**(2014), 41-98.
[19] M.Biswas, H. Om, A new soft-thresholding image denoising method, *Procedia Technology*, **6**(2012), 10-15.
[20] M. Hosseini, A.N. Nilchi, Medical ultrasound image compression using contextual vector quantization, *Computers in biology and medicine*, **42**(2012), 743-750.
[21] M. Mobini, M.R. Faraji, Multi-scale gradient wavelet-based image quality assessmen, *Vis Comput.*, **40**(2024), 8713-8728.
[22] M.P. Ekstrom, Digital image processing techniques, *Academic Press*, **2**(2012).
[23] M. Shafieian, F. Negahban, M. Rahmanian, Various novel wavelet - based image compression algorithms using a neural network as a predictor, *Journal of Basic and Applied Research International*, **3**(2013), 280-287.
[24] N. Cao, Y. Liu, High-Noise Grayscale Image Denoising Using an Improved Median Filter for the Adaptive Selection of a Threshold, *Appl. Sci.*, **14(2)**(2024), 635.
[25] P. Sahoo, S. Soltani, A. Wong, A survey of thresholding techniques, *Computer Vision, Graphics, and Image Processing*, **41**(1988), 233-260.
[26] P. Tay, S. Acton, J. Hossack, A wavelet thresholding method to reduce ultrasound artifacts, *Computerized medical imaging and graphics : the official journal of the Computerized Medical Imaging Society*, **35**(2010), 42-50.
[27] R. Gonzalez, Z. Faisal, Digital Image Processing Second Edition, (2019).
[28] R. Jain, P. Johari, An improved approach of CBIR using color based HSV quantization and shape based edge detection algorithm, *IEEE International Conference on Recent Trends in ELectronics Information Communication Technology*, (2016), 1970-1975.
[29] R. Mathar, M. Dorpinghaus, Threshold optimization for capacity-achieving discrete input one-bit output quantization, *IEEE International Sysmposium on Information Theory*, (2013), 1999-2003.
[30] S. Karthika, P. Rathika, An adaptive data compression technique based on optimal thresholding using multi-objective PSO algorithm for power system data, *Applied Soft Computing*, (2023).
[31] S. Mallat, A wavelet tour of signal processing, *Elsevier/Academic Press*, (2009), 535-606.
[32] S. Malviya, N. Gupta, An improved image compression algorithm based on Daubechies- wavelets with arithmetic coding, *JIEA*, **3(6)**(2013), 46-50.
[33] S. Raja, A. Suruliandi, Performance evaluation on EZW and WDR image compression techniques, *IEEE ICCCCT*, (2010), 661-664.
[34] S. Rajankar, O. Rajankar, S. Talbar, V. Raut, Signal Adaptive Threshold for ECG Signal Compression Using False Discovery Rate Approach, *Circuits Syst Signal Process*, **43**(2023), 5065-5089.
[35] T.V. Chang, S. Seibt, B. Von Rymon Lipinski, Hierarchical Histogram Threshold Segmentation - Auto-terminating High-detail Oversegmentation, *Proceedings of the IEEE/CVF Conference on Computer Vision and Pattern Recognition (CVPR)*, (2024), 3195-3204.
[36] V. Bruni, D. Vitulano, Combined image compression and denoising using wavelets, *Signal Processing: Image Communication*, **22**(2007), 86-101.
[37] V. S. Nguyen, M. H. Tran, H. M. Vu, A Research on 3D model construction from 2D DICOM, *International Conference on Advanced Computing and Applications (ACOMP), Can Tho, Vietnam*, (2016), 158-163.
[38] W.C. Siu, K.-C. Hui, Extended analysis of motion-compensated frame difference for block-based motion prediction error, *IEEE Trans Image Process*, **16(5)**(2007), 1232-1245.
[39] Y. Sun, L. Liping, Research on wavelet base selection in infrared image fusion, **6**(2010), 3823-3832.
[40] Y. Wang, X. Li, Y. Zhao, J.-F. Zhang, Threshold Selection and Resource Allocation for Quantized Identification, *J Syst Sci Complex*, **37**(2024), 204-229.
[41] Z. Ming, Y. Hu, W. Zhou, X. Zheng, C. Yao, D. Feng, ADTopk: All-Dimension Top-k Compression for High-Performance Data-Parallel DNN Training, *In Proceedings of the 33rd International Symposium on High-Performance Parallel and Distributed Computing (HPDC '24). Association for Computing Machinery, New York, NY, USA.*, (2024), 135-147.